Astronomy & Astrophysics manuscript no. 47696corr
November 3, 2023

Letter to the Editor

Two-dimensional MHD modelling of switchbacks from jetlets in the slow solar wind

Ruggero Biondo[1], Alessandro Bemporad[1], Paolo Pagano[2, 3], and Fabio Reale[2, 3]

[1] INAF-Turin Astrophysical Observatory, via Osservatorio 20, I-10025 Pino Torinese (TO), Italy
[2] Physics and Chemistry Department, University of Palermo, Piazza del Parlamento 1, I-90134 Palermo, Italy
[3] INAF-Palermo Astronomical Observatory, Piazza del Parlamento 1, I-90134 Palermo, Italy

November 3, 2023

ABSTRACT

Solar wind switchbacks are polarity reversals of the magnetic field, recently frequently measured by Parker Solar Probe inside 0.2 AU. In this letter we show that magnetic switchbacks, similar to those observed by PSP, are reproduced by injecting a time-limited collimated high-speed stream in the Parker spiral. We performed a 2D magnetohydrodynamics simulation with the PLUTO code of a slightly inclined jet at 1000 km/s between 5 and 60 $R_{\odot}$. The jet rapidly develops a field inversion at its wings and, at the same time, it is bent by the Parker spiral. The match with the radial outward wind field creates two asymmetric switchbacks, one that bends to the anti-clockwise and one that bends to the clockwise direction in the ecliptic plane, with the last one being the most extended. The simulation shows that such S-shaped magnetic features travel with the jet and persist for several hours and to large distances from the Sun (beyond 20 $R_{\odot}$). We show the evolution of physical quantities as they would be measured by a hypothetical detector at a fixed position when crossed by the switchback, for comparison with in situ measurements.

1. Introduction

One of the initial remarkable measurements (Velli et al. 2020; Raouafi et al. 2023) obtained by the Parker Solar Probe (PSP; Fox et al. 2016) during its first orbit around the Sun revealed the presence of exceptionally large and intermittent amplitude oscillations in the radial magnetic field. They are associated with jets of plasma and enhanced Poynting flux, interspersed in a smoother and less turbulent flow with near-radial magnetic field, with a duration going from seconds to tens of minutes (e.g. Bale et al. 2019; Kasper et al. 2019; de Wit et al. 2020; Rouillard et al. 2020; Schwadron & McComas 2021). These reversals of magnetic field do not correspond to crossings of the heliospheric current sheet, as demonstrated by the permanence of the electron pitch angle (Bale et al. 2019; Velli et al. 2020), but instead they are rapid S-shaped folds in the magnetic field. They are called switchbacks.

By looking at the temporal profiles of in situ data, it can be seen how the fluctuations in radial velocity δv_R are correlated to those of δB_R, corresponding to outward-propagating Alfvén waves. Additionally, the magnitude of the total magnetic field is almost constant, suggesting that the compressibility of the fluctuations is very small (Velli et al. 2020). Switchbacks are spherical-arc, polarized, large-amplitude Alfvén waves (Matteini et al. 2019). These waves have one interesting property: in correspondence to a magnetic field with an S-shaped fold, the radial component of the velocity must always show a positive enhancement, that is, a radial jet (Raouafi et al. 2023; Velli et al. 2020; Matteini et al. 2019).

Before PSP observations, magnetic switchbacks had been studied at 1 AU in fast solar wind from coronal holes (e.g. Kahler et al. 1996), beyond 1 AU with Ulysses (e.g. Balogh et al. 1999; Neugebauer & Goldstein 2013), and within 1 AU with the Helios probes (Borovsky 2016; Horbury et al. 2018). However, extensive measurements by PSP suggest that the presence of switchbacks increases drastically near the Sun (Bale et al. 2019; Kasper et al. 2019). These strong deviations from the Parker spiral-like magnetic field are observed in correspondence to increases in radial solar wind speed (Michel 1967) and are associated with pulsed or one-sided Alfvénic fluctuations (Gosling et al. 2009; Gosling et al. 2011). In PSP measurements this one-sided feature is especially clear: if the magnetic field rotates more than 60°, then its tangential component B_T is always positive and the tangential proton velocity v_T always exceeds 33 km/s (Kasper et al. 2019). These large transverse flows far exceed those considered by the axisymmetric Weber & Davis (1967) model, in which $v_T(r_A) < 0.1\Omega_{\odot} r_A$ (Kasper et al. 2019; Schwadron & McComas 2021): for $r_A = 15\ R_{\odot}$, it should be $v_T(r_A) < 3$ km/s according to Weber & Davis (1967). One-sided transverse flows are key observables from PSP that any theoretical formulation of switchbacks must explain (Schwadron & McComas 2021).

The mechanisms responsible for generating the switchbacks are under debate. It is not clear whether they are self-consistently generated in the solar wind (Squire et al. 2020; Shoda et al. 2021) or driven by lower solar atmosphere processes (Magyar et al. 2021). Their average occurrence features observed by PSP suggest a possible source in the coronal transition region rather than in situ (Bale et al. 2021; Fargette et al. 2021; Mozer et al. 2021); nevertheless, different models have been proposed. Switchbacks could be either a signature of magnetic reconnection events in the solar corona (e.g. Fisk & Kasper 2020; Zank et al. 2020) or they could be geometrical effects associated with the motion of coronal magnetic field footpoints from slow to fast solar wind sectors (Schwadron & McComas 2021). They could be Alfvénic structures originating in the low corona and propagating outwards into interplanetary space, as suggested by magnetohydrodynamics (MHD) simulations (see e.g. Matteini et al. 2015; Jakab & Brandenburg 2021) or they could be related to dynamics driven by velocity-shear instabilities (Landi et al. 2006; Ruffolo et al. 2020).

It is interesting to look at the conditions for ripples in the radial magnetic field to develop during the wind stream propagation in the heliosphere. Recently, Kumar et al. (2023) explored the possibility that switchbacks observed in the the outer corona and heliosphere could be a product of quasi-periodic jets and jetlets generated by interchange reconnection at the base of plumes and throughout coronal holes. By comparing the frequencies of switchback patches in the PSP measurements and that of co-temporal observations of jetlets made by the Atmospheric Imaging Assembly on board the Solar Dynamics Observatory (SDO/AIA; Lemen et al. 2012), they found a good agreement in their periodicity, as well as compositional signatures at PSP distances compatible with coronal jets.

In this work we model the transient deformation of the interplanetary magnetic field due to the propagation of disturbances expelled from the low corona. We simulate the propagation of a collimated jet of plasma into a uniformly filled Parker spiral solar wind, and show how this produces several inversions in the magnetic field direction, with sigmoidal shapes that closely resemble magnetic switchbacks.

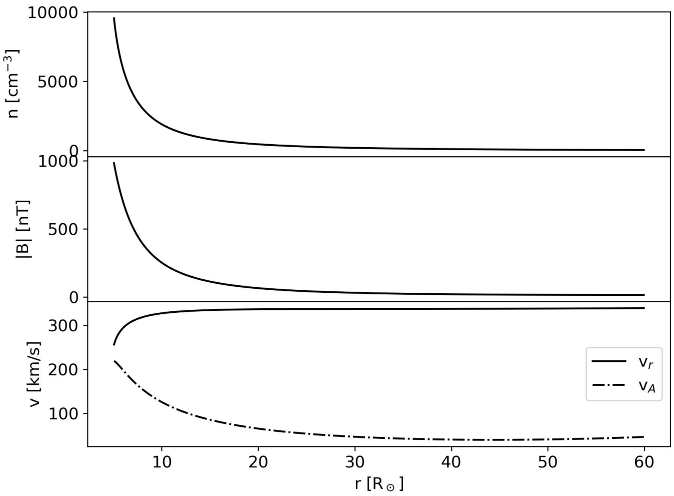

Fig. 1. Simulation initial conditions. From top to bottom are shown the radial profiles of particle number density, magnitude of magnetic field, plasma speed, and Alfvén speed. These are the same at all domain longitudes.

2. The model

The goal of the simulation is to reproduce the sigmoidal features of the magnetic field in switchbacks from the propagation of collimated jets from the lower corona.

We used the PLUTO code (Mignone et al. 2007, 2012) to solve the ideal MHD equations in a 2D spherical uniform grid (r, ϕ) corotating with the solar equator at $\Omega_\odot = 2.67 \cdot 10^{-6}$ rad s^{-1}:

$$\frac{\partial \rho}{\partial t} + \nabla \cdot (\rho \mathbf{v}) = 0, \tag{1a}$$

$$\frac{\partial (\rho \mathbf{v})}{\partial t} + \nabla \cdot \left[\rho \mathbf{v}\mathbf{v} - \mathbf{B}\mathbf{B} + \left(p + \frac{B^2}{2}\right)\right] = \mathbf{F_{rot}} - \rho \nabla \Phi, \tag{1b}$$

$$\frac{\partial \mathcal{E}}{\partial t} + \nabla \cdot \left[(\mathcal{E} + p + \frac{B^2}{2} + \rho\Phi)\mathbf{v} - \mathbf{B}(\mathbf{v}\cdot\mathbf{B})\right] = \mathbf{v} \cdot \mathbf{F_{rot}}, \tag{1c}$$

$$\frac{\partial \mathbf{B}}{\partial t} - \nabla \times (\mathbf{v} \times \mathbf{B}) = 0, \tag{1d}$$

where ρ is the plasma density, $\mathbf{v}$ its velocity, $\mathbf{B}$ the magnetic field, and p the plasma pressure; $\mathbf{F_{rot}}$ includes the Coriolis force and the centrifugal terms; Φ is the solar gravitational potential; and $\mathcal{E}$ is the total energy density, given by

$$\mathcal{E} = \frac{p}{\gamma - 1} + \frac{1}{2}\rho v^2 + \frac{B^2}{2} \tag{2}$$

with $\gamma = \frac{5}{3}$ being the specific heats ratio. The term $\mathbf{F_{rot}}$ is proportional to $\Omega_\odot$ and is ultimately responsible for the formation of the Parker spiral in the modelled wind.

The computational grid spans from 5 $R_\odot$ to 60 $R_\odot$ in the radial direction, using 512 cells of uniform length, and 0° to 30° in the longitudinal direction with 256 cells, also uniform. The boundary conditions are chosen as follows. On both sides of the longitudinal direction, conditions of periodicity are imposed. At the outer radial boundary, a zero gradient across the boundary is imposed, resulting in an outflow of quantities. At the inner (r=5 $R_\odot$) boundary, uniform conditions of inflowing slow solar wind are assumed along φ: density 10^4 cm^{-3}; temperature 1.5 MK; solar wind speed 250 km/s; magnetic field 10^3 nT. The computational domain is thus initially filled from the inner radial boundary with these longitudinally uniform values. Solving the MHD equations (1), we let the plasma and magnetic field flow from the inner boundary at 5 $R_\odot$ to the outer one at 60 $R_\odot$, to reach a longitudinally uniform steady state in about 20 days: the density, thermal pressure, and radial magnetic field decay as r^{-2}; the radial speed shows a Parker-like acceleration; and the longitudinal component of magnetic field forms a Parker spiral (see fig. 1). This stationary state is then used as initial condition to model the propagation of a transient perturbation that produces switchback-like features.

The collimated jet propagating from the lower corona is described as a bounded perturbation consisting of a time-limited fast plasma stream injected as a time-dependent condition at the lower radial boundary. Here, we are not interested in modelling a completely realistic coronal jet, but rather the features generated in the solar wind at heliocentric distances comparable with those crossed by PSP, by a perturbation like the one described below. To represent a generic orientation, the perturbation is not injected perfectly aligned with the radial direction. We chose an angle of 10° with respect to the radial direction. At 5 $R_\odot$ in the longitudinal interval between 17.5° and 18°, the plasma speed is multiplied by a factor of 4, corresponding to a speed of 1000 km/s, for a time interval of nearly 18 minutes. While this is an atypical speed for a coronal jet, and closer to that of a strong streamer puff (see e.g. Bemporad et al. 2005), this perturbation is merely used to kick the initial instability, and it is soon slowed down by the background medium. The φ-interval is chosen above the midpoint of the longitudinal domain (15°) so that the stream propagates close to it, since in the frame of reference corotating with the Sun the stream drifts westwards, as it rotates with the Parker spiral. The initial values of density, temperature, and magnetic field of the jet are the same as those in the unperturbed medium. The increased plasma velocity at the lower boundary departs from the initial steady state wind solution and such transient also induces changes in density and pressure, whose evolution is modelled numerically with the Linearized Roe Riemann (Roe 1986) solver for the MHD equations used in PLUTO.

3. Results

In the very first phases of its propagation, between $t = 0$ and $t = 3.0$ h, the jet travels outwards, losing speed and drifting westwards due to the solar rotation. At the same time, it drags and stretches the magnetic field, compressing it and enhancing its strength inside the flow and decompressing it in the immediate surroundings. The jet blows away the plasma near the injection point, forming a low-density region at its head. A dense bow shock front precedes the jet. As the fast thin wind stream propagates in the denser, slower medium, it is slowed down and starts to blur. At a distance of a few $R_\odot$, the stream travels faster than the local Alfvén speed and the magnetic field is significantly warped by it and lags behind, thus determining a reversal of its sign. Due to the Parker spiral rotation, the stream gradually bends westwards, and makes the warping asymmetric as well, until only the westward warp is detectable.

Figure 2 shows four maps of the simulation results at four successive and representative times: equatorial maps of the difference between the particle number density n at time t and at time $t = 0$ (first column), the radial speed v_r (second column), the radial component of magnetic field B_r (third column), and the difference between t and $t = 0$ of the longitudinal component of magnetic field B_φ (fourth column), normalized to the unperturbed value, at $t = 3.19, 3.82, 4.3$, and 8.46 hours from the insertion time of the perturbation.

At $t = 3.19$ h, the flow has reached a distance beyond 12 $R_\odot$ and is clearly bent eastwards. The dense bow shock precedes the jet, which is instead at low density, but at a speed above 700 km/s at its head. There are two regions where the radial component of the magnetic field has a clear inversion, on the two sides of the jet head. Due to the jet bending caused by the Parker spiral rotation, the region on the west side is more extended, while, the region on the east side of the perturbation is thinner in size. Coherently, significant B_φ components are present, both where the bow shock perturbs the field, and where the inverted field connects back to the background unperturbed field.

Times $t = 3.82$ h and $t = 4.3$ h show that the stream moves forwards, and maintains its structure, although slightly weakening in density and velocity. The field inversion is also maintained, although it becomes weaker as well. The motion will have important effects on hypothetical in situ measurements, as shown in Fig. 3.

The resulting asymmetry of the simulated switchbacks is consistent with the findings of Fargette et al. (2022), who observed a systematic bias of these deflections towards the rotational direction of the Parker spiral (that is, in the clockwise direction of the panels in fig. 2) regardless of the main magnetic field polarity. The authors also found a slight latitudinal bias, also independent of magnetic polarity, which causes the majority of switchbacks to lean towards the equator.

The weakening of both the stream and the magnetic field inversion slows progresses as the stream propagates to larger distances. At t = 8.46 h and a distance of about 24 $R_\odot$, the magnetic field is still distorted, although the flow is barely visible. We obtain similar results for different initial values of density, speed, and duration of the initial perturbation. We invariably find switchbacks and the dependence on the initial perturbation is weak. In general, a jet with larger momentum generates a stronger shock and a longer-lasting switchback.

Figure 3 shows time profiles of plasma quantities and magnetic field taken at the heliocentric distance of 13.3 solar radii and at a longitude around 15° (i.e. close to the centre of the perturbation) and at a distance comparable to that of the PSP perihelia of encounters 10 to 16, as labelled in Fig. 2. The position is one where the radial component of the magnetic field has a large negative value, but the profiles do not vary much moving clockwise in φ around this point. Instead, moving in the opposite direction in φ, east of the jet, it is possible to detect the anticlockwise switchback as a shorter magnetic inversion of similar entity.

As also shown in Fig. 2, the bow shock is intercepted at the position at $t \sim 3.2$ hours from the jet insertion time, with clear steep fronts in density, radial velocity and pressure. The density has a peak, but then rapidly decreases below the background value because we measure the underdensity around the jet, and the small dip at $t \sim 4.3$ h is exactly the jet itself. Thereafter, the density gradually grows in the wake of the jet and recovers to the background value at $t \sim 7$ h. The velocity has no initial peak because the plasma uniformly propagates in the post-shock, but we find a later peak at $t \sim 4.3$ h which again indicates that the jet itself is crossing. After this the velocity gradually recovers again to the background value. The pressure also has an initial peak, but then it decreases much more gradually than the density, and shows a clear dip as the jet passes through.

The two bottom panels show the evolution of the magnetic field components. The radial component shows the expected field inversion as a low flat minimum at negative values (above -60 nT) between $t \sim 3.6$ h and $t \sim 4.2$ h. This is the main signature of the switchback. The component rises back to a maximum at the unperturbed value and shows another smaller dip, which is another smaller deformation in the rear side of the jet. The B_φ component shows a coherent and complementary evolution: it is positive as the shock passes, and then goes back to zero; it marks the field warping afterwards with a minimum and a maximum, and then recovers to the small unperturbed value.

4. Conclusions

Observations collected by Parker Solar Probe in the near-Sun solar wind have shown an unexpected abundance of fluctuations in its density and speed, associated with polarity-reversing folds in the interplanetary magnetic field. The origins and sources of these switchbacks in the solar wind are still not fully understood, nor is the role they may play in the solar wind acceleration, its heating, and its turbulent cascade (see e.g. Raouafi et al. 2023).

Among the possible explanations for the switchback birthing mechanism, the rearranging of open magnetic field lines with a closed magnetic loop, known as interchange reconnection (e.g. Fisk & Kasper 2020; Wyper et al. 2022), has been considered a good candidate by different authors (Raouafi et al. 2023). This fact, and that the occurrence of switchbacks does not appear to depend on radial distances (Mozer et al. 2021), and also the fact that they occur in patches, (which could be related to solar granulation and super-granulation, see e.g. Bale et al. 2019; Fargette et al. 2021), seem to point to a coronal origin (Jagarlamudi et al. 2023). Kumar et al. (2023) demonstrated that the periodicity of switchbacks in radial velocities is consistent with that observed in the extreme-UV emissions of jetlets at the base of plumes and in coronal holes.

In this letter we have presented the results of an MHD simulation of a collimated jet of plasma coming from the corona and travelling in the slow solar wind between 5 and 60 solar radii. We showed how this perturbation interacts with the background medium, by switching the magnetic field polarity of the solar wind while propagating in a super-Alfvénic region, and bends its magnetic field lines to form persistent solar wind switchbacks.

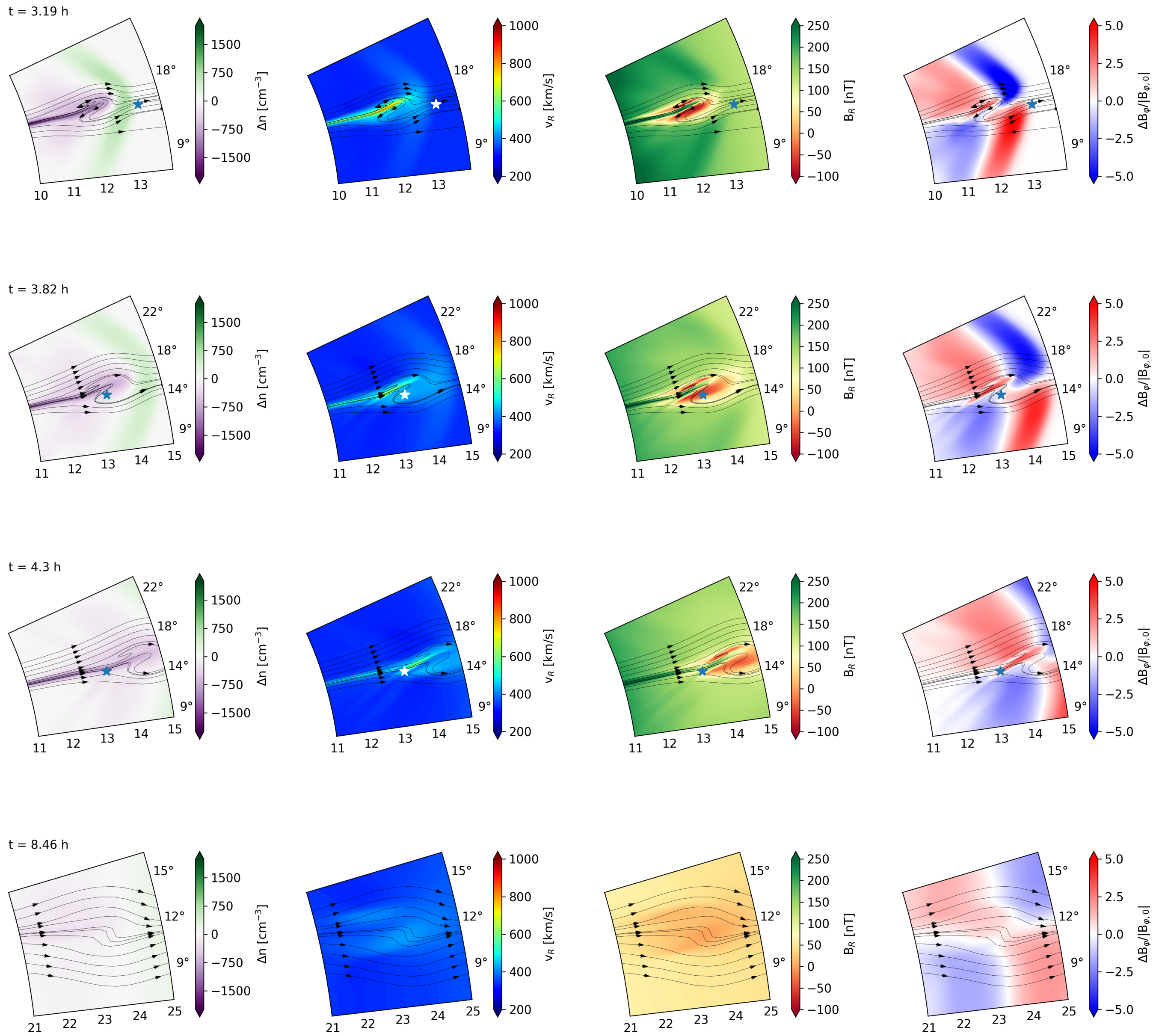

Fig. 2. Close-ups of the propagation of a faster jet of plasma in a uniform medium at different times from the insertion time $t = 0$: $t = 3.19, 3.82, 4.3, 8.46$ h. From left to right in each row: Difference between the particle density n at time t and its initial value at $t = 0$, the wind radial velocity v_r, the radial component of magnetic field B_r, and the difference between the longitudinal magnetic field B_φ at time t and that at time $t = 0$, normalized by the initial absolute value of B_φ. A selection of magnetic field lines drawn near the centre of the perturbation are included (black arrowed lines). The position where the time profiles of Fig. 3 are taken is given (star). An animation is attached.

The main observed signature of switchbacks, that is, the inversion of magnetic field co-temporal with enhancements in solar wind speed, is correctly captured by our model, thus showing that fast jets could in principle generate this feature as detected in situ by spacecraft close to the Sun such as PSP and Solar Orbiter, or at Earth's orbit.

While the fast stream produces switchbacks with opposite orientations as it propagates, this symmetry is broken by the rotation of the Parker spiral, resulting in a wider region of magnetic warp west of the jet, and a narrow one east of it. This could explain the observed preferential orientation of switchbacks, which is in the clockwise direction of the ecliptic plane regardless of magnetic polarity (Fargette et al. 2022); anti-clockwise switchback patches might have a significantly smaller spatial extension, a shorter duration, and could thus be difficult to observe. Squire et al. (2022) similarly showed with analytical arguments that the preferential direction of the magnetic field rotations in switchbacks is a consequence of the propagation of arc-polarized MHD waves in the Parker spiral, regardless of their generation mechanism.

It is also worth noting that the transient we simulated is not expected to result in the remote sensing observations as an S-shaped propagating feature, because the density perturbation does not match the field reversal. This feature will appear in-

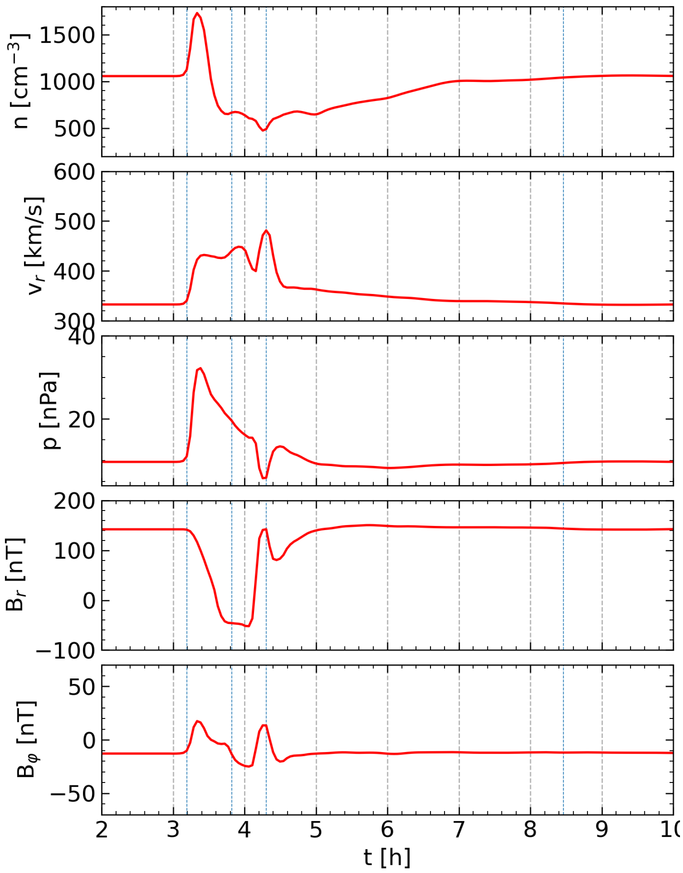

Fig. 3. Time profiles taken approximately at 13.3 solar radii and φ =15°. From top to bottom are shown the profile of particle number density, radial speed, plasma pressure, and the radial, and longitudinal components of magnetic field. The perturbation front reaches 13.3 $R_\odot$ in approximately 3.2 hours from its insertion time, while the switchback itself, identified with increase in radial speed and the polarity reversal of magnetic field, follows shortly after. The four vertical blue dashed lines mark the corresponding snapshots shown in fig. 2.

stead as propagating arch-shaped compression wave, followed by a narrower density depleted region. The high-cadence observations now provided by the Metis coronagraph (Antonucci et al. 2020) on board Solar Orbiter should be able to capture similar phenomena propagating in the solar corona.

While our model can reproduce the magnetic field reversals and the corresponding velocity enhancements associated with switchbacks, it remains a two-dimensional representation trying to describe a three-dimensional phenomenon. This becomes clear when considering the magnetic field behaviour, which in our simulation has no latitudinal component. In spite of this, we can reproduce the abrupt decrease in the magnetic pressure that the observed switchback shows (Bale et al. 2019; Farrell et al. 2020). Future works employing full-3D simulations, and more realistic solar wind models, might help in improving the agreement with in situ observations.

Acknowledgements. The authors acknowledge support from ASI/INAF agreement n. 2018-30-HH.1-2022 and from INAF "Theory Grant" n. 1.05.12.06.09. Computations were performed on the CORVUS cluster at the SCAN (Sistema di Calcolo per l'Astrofisica Numerica) facility for high-performance computing at INAF-Palermo Astronomical Observatory.

References

Antonucci, E., Romoli, M., Andretta, V., et al. 2020, A&A, 642, A10 4
Bale, S. D., Badman, S. T., Bonnell, J. W., et al. 2019, Nature, 576, 237 1, 4
Bale, S. D., Horbury, T. S., Velli, M., et al. 2021, The Astrophysical Journal, 923, 174 1
Balogh, A., Forsyth, R. J., Lucek, E. A., Horbury, T. S., & Smith, E. J. 1999, Geophysical Research Letters, 26, 631 1
Bemporad, A., Sterling, A. C., Moore, R. L., & Poletto, G. 2005, ApJ, 635, L189 2
Borovsky, J. E. 2016, Journal of Geophysical Research: Space Physics, 121, 5055 1
de Wit, T. D., Krasnoselskikh, V. V., Bale, S. D., et al. 2020, The Astrophysical Journal Supplement Series, 246, 39 1
Fargette, N., Lavraud, B., Rouillard, A. P., et al. 2022, A&A, 663, A109 3, 4
Fargette, N., Lavraud, B., Rouillard, A. P., et al. 2021, The Astrophysical Journal, 919, 96 1, 4
Farrell, W. M., MacDowall, R. J., Gruesbeck, J. R., Bale, S. D., & Kasper, J. C. 2020, The Astrophysical Journal Supplement Series, 249, 28 4
Fisk, L. A. & Kasper, J. C. 2020, The Astrophysical Journal Letters, 894, L4 1, 4
Fox, N. J., Velli, M. C., Bale, S. D., et al. 2016, Space Sci. Rev., 204, 7 1
Gosling, J. T., McComas, D. J., Roberts, D. A., & Skoug, R. M. 2009, ApJ, 695, L213 1
Gosling, J. T., Tian, H., & Phan, T. D. 2011, The Astrophysical Journal Letters, 737, L35 1
Horbury, T. S., Matteini, L., & Stansby, D. 2018, Monthly Notices of the Royal Astronomical Society, 478, 1980 1
Jagarlamudi, V. K., Raouafi, N. E., Bourouaine, S., et al. 2023, ApJ, 950, L7 4
Jakab, P. & Brandenburg, A. 2021, A&A, 647, A18 1
Kahler, S. W., Crooker, N. U., & Gosling, J. T. 1996, J. Geophys. Res., 101, 24373 1
Kasper, J. C., Bale, S. D., Belcher, J. W., et al. 2019, Nature, 576, 228 1
Kumar, P., Karpen, J. T., Uritsky, V. M., et al. 2023, arXiv e-prints, arXiv:2305.06914 1, 4
Landi, S., Hellinger, P., & Velli, M. 2006, Geophysical Research Letters, 33 1
Lemen, J. R., Title, A. M., Akin, D. J., et al. 2012, Sol. Phys., 275, 17 1
Magyar, N., Utz, D., Erdélyi, R., & Nakariakov, V. M. 2021, The Astrophysical Journal, 911, 75 1
Matteini, L., Horbury, T. S., Pantellini, F., Velli, M., & Schwartz, S. J. 2015, ApJ, 802, 11 1
Matteini, L., Stansby, D., Horbury, T. S., & Chen, C. H. K. 2019, Nuovo Cimento C Geophysics Space Physics C, 42, 16 1
Michel, F. C. 1967, Journal of Geophysical Research (1896-1977), 72, 1917 1
Mignone, A., Bodo, G., Massaglia, S., et al. 2007, ApJS, 170, 228 2
Mignone, A., Zanni, C., Tzeferacos, P., et al. 2012, ApJS, 198, 7 2
Mozer, F. S., Bale, S. D., Bonnell, J. W., et al. 2021, The Astrophysical Journal, 919, 60 1, 4
Neugebauer, M. & Goldstein, B. E. 2013, in American Institute of Physics Conference Series, Vol. 1539, Solar Wind 13, ed. G. P. Zank, J. Borovsky, R. Bruno, J. Cirtain, S. Cranmer, H. Elliott, J. Giacalone, W. Gonzalez, G. Li, E. Marsch, E. Moebius, N. Pogorelov, J. Spann, & O. Verkhoglyadova, 46–49 1
Raouafi, N. E., Matteini, L., Squire, J., et al. 2023, Space Science Reviews, 219, 8 1, 4
Roe, P. L. 1986, Annual Review of Fluid Mechanics, 18, 337 2
Rouillard, A. P., Kouloumvakos, A., Vourlidas, A., et al. 2020, The Astrophysical Journal Supplement Series, 246, 37 1
Ruffolo, D., Matthaeus, W. H., Chhiber, R., et al. 2020, The Astrophysical Journal, 902, 94 1
Schwadron, N. A. & McComas, D. J. 2021, The Astrophysical Journal, 909, 95 1
Shoda, M., Chandran, B. D. G., & Cranmer, S. R. 2021, The Astrophysical Journal, 915, 52 1
Squire, J., Chandran, B. D. G., & Meyrand, R. 2020, The Astrophysical Journal Letters, 891, L2 1
Squire, J., Johnston, Z., Mallet, A., & Meyrand, R. 2022, Physics of Plasmas, 29, 112903 4
Velli, M., Harra, L. K., Vourlidas, A., et al. 2020, A&A, 642, A4 1
Weber, E. J. & Davis, L. J. 1967, ApJ, 148, 217 1
Wyper, P. F., DeVore, C. R., Antiochos, S. K., et al. 2022, ApJ, 941, L29 4
Zank, G. P., Nakanotani, M., Zhao, L.-L., Adhikari, L., & Kasper, J. 2020, The Astrophysical Journal, 903, 1 1